PRODUCTION OF NEGATIVE PIONS OF MEDICAL INTEREST BY HIGH-ENERGY PROTONS*

D. Berley, L.N. Blumberg, D.C. Bonar, R. Fairchild, J.D. Fox, W-C Lam, D.M. Lazarus
Y.Y. Lee, C.L. Wang, Brookhaven Nat'l Laboratory, Upton, L.I., N.Y.

A.S. Kanofsky, Lehigh U., Bethlehem, Pa., W.T. Chu, Loma Linda U., Loma Linda, Calif.
M. Blecher, Virginia Poly. Inst. & State U., Blacksburg, Va.

Abstract

Improvements in intensity and availability of extracted proton beams from high energy accelerators lead to the possibility of forming negative pion beams useful for treating deep-seated cancers.[1] To optimize pion fluxes and design parameters for such beams, an experiment was performed at the Brookhaven Alternating Gradient Synchrotron to measure yields of negative pions produced by protons of 6 to 17 GeV/c incident on targets of different thickness and material. Measurements were made at production angles between 0° and 30° for pion momenta from 150 to 350 MeV/c. A dose rate of 24 rads/min in a 100 cm^2 field is attainable at the Alternating Gradient Synchrotron of the Brookhaven National Laboratory.

Introduction

It has now become possible to treat deep-seated tumors with charged particle radiotherapy. Negative pions are particularly attractive for this application as the Bragg peak at the end of their range is enhanced by the disintegration of the nuclei into which the negative pions are captured. This results in a large ratio of dose at the end of the range (at the tumor) to that delivered to healthy tissue through which the particles pass in reaching the tumor. Interest in radiotherapy using negative pions has recently been stimulated by estimates of the π^- fluxes expected at the Los Alamos Meson Physics Facility (LAMPF) when it comes into operation and presently available at the AGS.

The only published measurement of the production of negative pions with momentum below 500 MeV/c at a multi-GeV accelerator is that of Fitch, Meyer and Piroué[2] who obtained .09 and .05 π^- per steradian per GeV/c per circulating proton produced at 45° and 90° respectively, relative to the beam incident on the internal target at the AGS. More recently a measurement of 200 MeV/c π^- production has been made at the AGS at 18.8° to the internal target[3] which gave a production of .1 - .4 π^- per steradian per GeV/c per interacting proton.

No data exist regarding the enhancement of low-energy pion production by nuclear cascade although the effect is expected, and the expectation is supported by a Monte Carlo calculation[4].

The useful negative pion intensity that can be delivered to a tumor with minimum damage to surrounding healthy tissue depends, of course, on the beam transport to the patient, as well as the pion production. However, the beam parameters can be calculated to an adequate level of precision whereas it is at present important to have a better knowledge of the production cross section, $\frac{\partial^2 N}{\partial p \partial \Omega}$, and the cascade enhancement.

We have measured the negative pion production by protons in the pion momentum range 150 MeV/c to 350 MeV/c at three proton momenta, 6, 12 and 17 GeV/c. Data was obtained at four production angles from 0° to 30° for three target materials Al, Cu and W. The dependence of pion yield on target length was investigated.

Experiment

The measurements were carried out in the East Test Beam at the AGS. The beam is at 4.7° to the internal target and it transported 10^5 to 10^6 protons per AGS cycle to our production target. The protons in this beam were available over a momentum range of 5 to 17 GeV/c with a transmitted momentum band of $\pm$ 2%. The experimental arrangement is shown in Fig. 1. The protons were incident on the production target after passing through the Cerenkov counter, filled with Freon 12, which identified positive pions in the beam, and the three beam counters S_1, S_2, S_3 which were smaller in transverse dimensions than the target and therefore defined the target area through the trigger requirement. Cerenkov counter efficiency measurements indicated that less than one percent of the triggers were on positive pions in the beam. Secondary particles produced in the target were momentum analyzed by the 72D18 (72-in. by 18-in. by 12-in. gap) spectrometer magnet and four pairs of scintillation counter hodoscopes. The spectrometer magnetic field was mapped both in and out of the median plane. The floating wire technique was used as a momentum calibration determining the positions of the hodoscopes. The secondary particles were bent through 30°.

Each hodoscope pair consisted of an upstream array of three 1-in. by 3-in. scintillation counters U_1, U_2, U_3 and a downstream array of four 2-in. by 8-in. counters D_1 - D_4 as shown in Fig. 2. Each combination of counters U_i D_j gives an angular resolution of 1.8° corresponding to a momentum resolution $\frac{\Delta p}{p}$ = .06. The event trigger used in the experiment was

$$S_1 . S_2 . S_3 . \bar{C} . U_i . D_j . D_t$$

where j = i or i + 1

This produced a momentum acceptance $\frac{\Delta p}{p}$ = 12%. The region between the target and the downstream hodoscopes was enclosed in a system of helium bags in order to reduce multiple Coulomb scattering. Negative secondary particles were identified by their time of flight for the 16-ft trajectory between the beam counter S_3 and a 2-in. by 8-in. scintillation counter placed immediately behind each downstream hodoscope D_t. Peaks in the time of flight spectra corresponding to electrons and negative pions were observed. In order to separate the peaks cleanly, the outputs of the beam timing counter S_3 (XP1020 photomultiplier tube) and the downstream timing counters D_t (56AVP photomultiplier) were clipped and zero crossing discriminators were used. The 8-in. length of the scintillators in the downstream timing counters would introduce a 2/3 nanosec difference in transit time between particles incident at the end near the photomultiplier and those incident at the far end. This was reduced by using the downstream hodoscope counters D_j to determine which half of the timing counter the particle passed through and introducing a suitable delay (.3 nanosec) between signals from the two halves before routing them to the time to amplitude converters (TAC). Simultaneous time of flight spectra were taken for the four hodoscopes and stored in a 1024 channel pulse height analyzer. A time of flight resolution of .6 nanosec was achieved. A 200 MeV/c spectrum for 10° production by 6 GeV/c protons is shown in Fig. 3.

Data and Analysis

Table I indicates the matrix of proton and pion momenta studied along with target information. The

*Work performed under the auspices of the U.S. Atomic Energy Commission.

data is tabulated in Table II.

In a given time interval the number of negative pions N_π detected in a downstream timing counter D_T is

$$N_\pi = N_p Y \,\Delta\Omega\, \Delta p \,\exp(-L/\gamma\beta c\tau) \qquad (1)$$

where N_p is the number of protons incident on the target in the time interval as defined by the beam counters, Y is the number of π^- produced in the target, $\Delta\Omega\Delta p$ is the acceptance of the hodoscope timing counter combination and the exponential factor is the decay factor, L being the time of flight path length, $c\tau$ the proper time decay length, 780.2 cm, for charged pions, $\gamma = (1-\beta^2)^{-\frac{1}{2}}$. The yield Y is then determined from the measurements of the other parameters in Eq. (1). N_p, the number of beam protons was corrected for accidentals by recording $S_1 S_2' S_3 \bar{C}$ where the prime indicates S_2 was timed out of coincidence with the other beam counters. The maximum accidental rate was 2% for the beam counters and the positive pion contamination was less than 1%.

The acceptance $\Delta\Omega\Delta p$ was computed with a Monte Carlo program which integrates the force equation along particle tranjectories through the field of the spectrometer magnet. A complete tabulation of the field of the spectrometer magnet was generated from the map of the vertical component of magnetic field in the median plane by symmetry and the requirements that curl B = 0 and div B = 0[5]. The large bending angle of 30° introduces large vertical focusing effects producing an increase in $\Delta\Omega\Delta p$ of up to 100% over the geometrical acceptance.

The largest uncertainty is in the number of pions detected. Although rate effects were negligible the large ratio of electrons to negative pions made background subtraction under the pion time of flight peak difficult especially at 0° and low secondary momenta where e^-/π^- ratios exceeding 100/1 were measured. Despite the good time resolution there were sufficient electrons in the wings of the time of flight distribution to cause considerable uncertainty in the determination of the pion component. This was complicated by those muons arising from decay in flights of pions somewhere along the trajectory. Monte Carlo calculations indicated a maximum of 7% of the pion peak might be muons which would be indistinguishable from pions. Generally this contamination is less than 5% but these muons appear in between the pion and electron peaks in the time of flight spectra and are impossible to distinguish. Accidentals in the time of flight spectra are generally less than 1%. The background subtraction was independently carried out by three physicists and the errors assigned reflect the consistency of their estimates. In general this produced a larger uncertainty in the results than counting statistics.

Discussion of Results

The results of our measurements are summarized in Figs. 4 - 6, where the dependences of π^- production on incident proton momentum, pion momentum and on target thickness are shown. The thick target effects are the following:

1) Nucleon-meson cascade production: The high-energy secondaries produced by each interacting proton will interact with other nucleons in the target to produce tertiaries, etc.

2. Target as degrader: Pions undergo appreciable energy loss in the target and the observed pions must therefore have been produced at higher momentum, and thus with higher probability.

3) Self-absorption by the target, which removes low momentum pions from the beam, is an increasing function of target thickness.

4) Multiple-scattering which is also an increasing function of target thickness, tends to obscure the angular dependence of pion production.

Measurements were made to investigate the "thick target effects" for the production of 200 MeV/c pions. Figure 4 shows that at an incident proton momentum of 6 GeV/c, 6-in. of Cu is the optimum target thickness. The same thickness is almost optimum for 17 GeV/c incident protons. The angular variation plot of Fig. 5 shows that for a thick target negative pion production is nearly isotopic over our range of measurement. However, the e^-/π^- ratio drops rapidly with increasing angle. Figure 6 shows that for 6-in. Cu target, pion yield increases with both pion momentum and incident proton momentum.

In order to extrapolate to higher AGS energies, smooth curves were drawn through data points for 6, 12, and 17 GeV/c incident proton momenta and then the yield was plotted as a function of proton momentum as shown in Fig. 7. It was then extrapolated linearly to 30 GeV/c. Figure 8 shows the dose rate obtainable from the AGS under the present operating conditions (6×10^{12} protons/sec) as a function of pion momentum computed for a hypthetical beam 10 m long of 25 msr acceptance. It is evaluated from the expression[4]

$$D = \frac{Y \cdot \Delta\Omega \cdot \Delta p \cdot \exp(-L/\lambda) \cdot f_s \cdot E_s}{AtC} \qquad (2)$$

where
- D = dose rate (rad/sec)
- L = beam length (10 m)
- λ = decay length for pions = $\gamma\beta c\tau$
- f_s = fraction surviving interactions in degrader before coming to rest
- E_s = energy deposited at end of stopping range (60 MeV) including Bragg peak ionization and the star resulting from pion capture
- A = cross section area of beam (100cm^2 for this calculation)
- t = longitudinal dimension of stopped pion region in tissue
- C = 6.25×10^7 MeV/g, assuming tissue density = 1 g/cm³ for this calculation
- Y = pion yield/sr/(GeV/c)/incident proton
- $\Delta\Omega$ = 25 msr geometrical acceptance
- Δp = pion momentum acceptance

The range spread, ΔR, which is a function of pion momentum is just the longitudinal dimension t of the tumor volume. If one parameterizes the range in a power law of T_π, pion kinetic energy, as $R = aT_\pi^n$, then

$$\Delta p = \frac{(T_\pi + m_\pi)}{p} \frac{t}{anT_\pi^{n-1}} \qquad (3)$$

where m_π and p are pion mass and momentum respectively.

The fraction of pions surviving interactions with degrader material is estimated with the expression

$$f_s = \exp\left[-N \int_0^T \sigma \, dT \Big/ \left|dT/dx\right|\right] \qquad (4)$$

where
- T = kinetic total energy of pion at entrance to degrader
- σ = total interaction cross-section
- N = number of atoms/cm³

We have assumed the degrader has the density of body tissues of 1 gm/cm³ with average properties equivalent to that of carbon. The resulting dose vs pion momentum relationship has a maximum at about 200 MeV/c with a rate of 24 rads/min in a field of 100cm^2. This dose rate is considered quite adequate for the clinical use of negative pi-meson in radiotherapy.

Table III lists the proton fluxes and dose rate from various accelerators in this country. At this time, the Los Alamos Scientific Laboratory is commited to a clinical trial of negative pion tumor therapy. When their 800 MeV proton linac operates at the design intensity of 6x10^{15} protons per sec., the biomedical channel would have a dose rate of 35 rads/min in a 100 cm^2 field[6]. A comparable flux of 24 rads/min would be obtainable from the AGS of the Brookhaven National Laboratory with the proton intensity which is available now. The pion fluxes available at the ZGS and Bevatron were computed on the basis of the pion yield data from this work and the maximum proton intensities as indicated. However, machine improvement programs are underway in all these laboratories; it is quite likely in the future that pion radiotherapy can be done at several locations around the nation.

Acknowledgment

We wish to thank H.L. Atkins, V.P. Bond, E.P. Cronkite and F.E. Mills for their interest and encouragement, and T.J. Blair for his assistance during the experiment. We are in debt to G. Bennett, G. Levine and W. Moore for their support. The interest of R. R. Rau was important for initiating this measurement. The excellent service from the AGS control room staff: J. W. Glenn, A. Watts, A. McGeary, G. Cornish and J. Gabusi was essential for the success of this experiment. The cooperation of D. Nygren and J. Christenson of the Columbia/NYU/CERN group was appreciated.

References

1. V.P. Bond, Am.J. Roentgenology, Radium Therapy and Nuclear Medicine <u>111</u>, 9 (1971).
2. V.L. Fitch, S.L. Meyer and P.A. Piroué, Phys. Rev. <u>126</u>, 1849, 1962.
3. D. Bassano, D.M. Lazarus and C.L. Wang, BNL Accelerator Dept. Int. Rpt. EP&S 71-6, 1972.
4. Proposal for the Use of the Brookhaven National Laboratory Alternating Gradient Synchrotron for Pi-minus Meson Therapy BNL 1971.
5. B. Zacharov, Nuc. Inst. and Meth. <u>33</u>, 136, 1965.
6. R.L. Hutson and M. Jakobson, "The LAMPF Biomed Pion Channel: a Preliminary Report," MP-7-34 (1971).

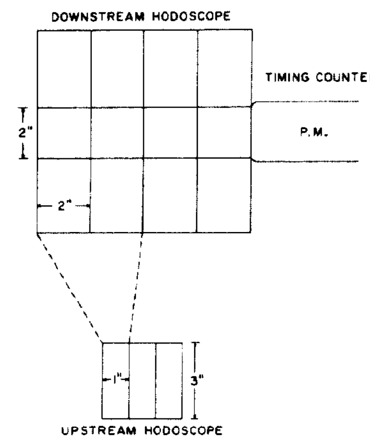

FIG.2 Configuration of one of the four hodoscope scintillator arrays. Upstream array consisted of 3 counters U_1, U_2, U_3. Downstream array consisted of 4 counters D_1, D_2, D_3, D_4 and a timing counter D_t. Acceptance is determined by 3 combinations of coincidence $U_i \cdot D_j \cdot D_T$ where j=i or i+1, i=1,2,3.

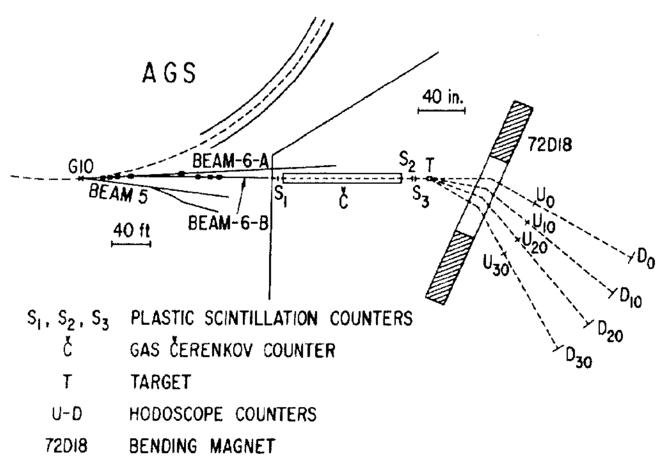

FIG.1 Plan view of experiment: Protons produced in the internal target at the AGS were transported in a beam through the proton telescope (plastic scintillators S_1, S_2, S_3 and Cerenkov counter Č) to the target T. Beam defining counter S_3 was 1.5" high by 1.25" wide. Target was 2"x2" in cross-section. Particles produced in T were then analyzed by the 72D18 spectrometer magnet and the hodoscope system U-D.

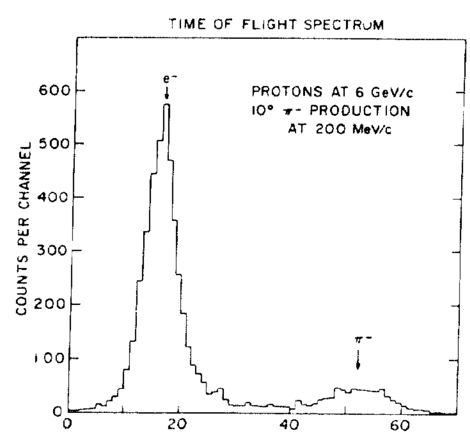

FIG.3 Time-of-flight spectrum for 200 MeV/c negative particles produced in a 3"Cu target by 6 GeV/c protons. The time scale is 10 channels per ns.

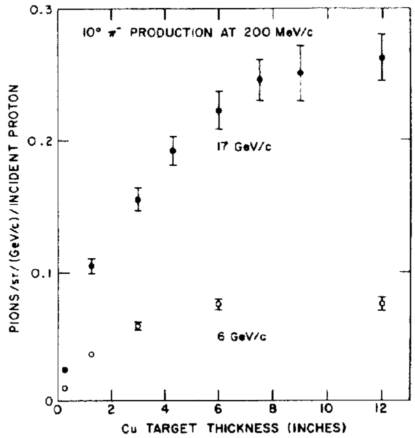

FIG.4. Negative pion production as a function of target thickness.

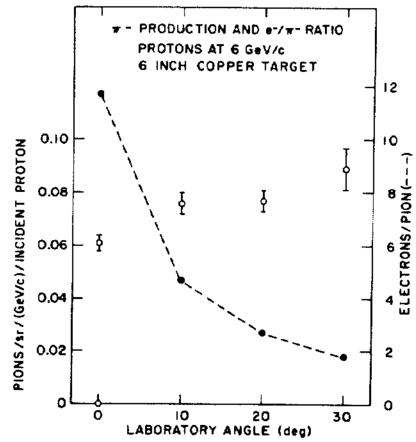

FIG.5 200 MeV/c negative pion production as a function of laboratory emission angle. The electron-pion ratio, measured at 16 ft flight path, is also presented.

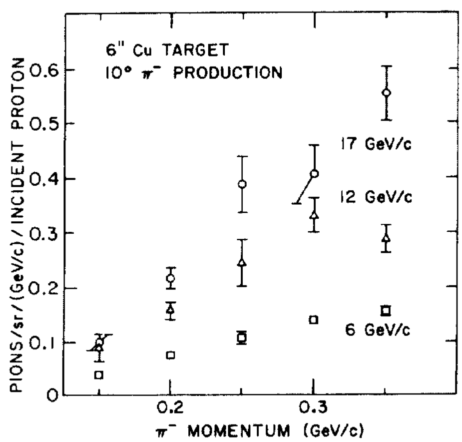

FIG.6 Negative pion momentum spectrum.

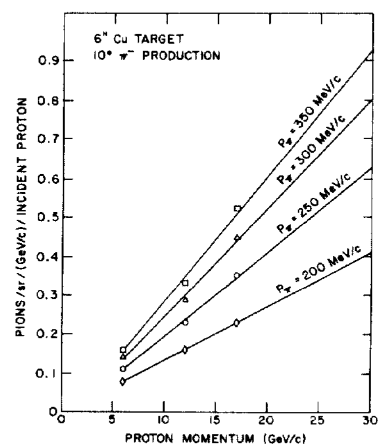

FIG.7 Negative pion production as a function of incident proton momentum derived from Fig. 6. Error bars are not shown.

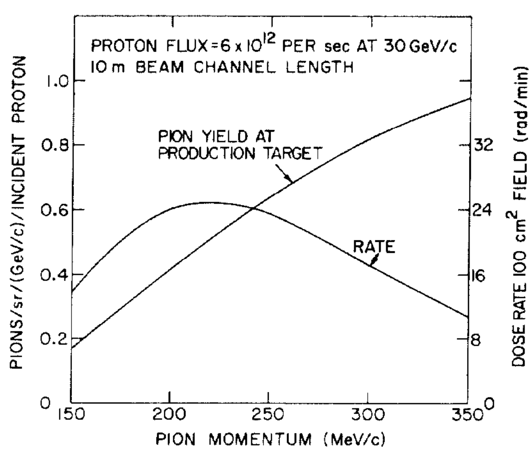

FIG.8 Negative pion flux and depth dose rate, estimated from data, and plotted as a function of pion momentum, for 100 cm^2 field.

TABLE I

Pion Momentum (MeV/c)	Proton Momentum (GeV/c): 6	12	17
150	Al(I), Cu(I), W(I)	Cu(I)	Al(I), Cu(I), W(I)
200	Al(I), Cu(L), W(I)	Cu(I), Cu(T)	Al(I), Cu(L), W(L)
250	A(I), Cu(I), W(I)	Cu(I)	Al(I), Cu(I), W(I)
300	Al(I), Cu(I), W(I)	Cu(I)	Al(I), Cu(I), W(I)
350	Al(I), Cu(I), W(I)	Cu(I), Cu(T)	Al(I), Cu(I), W(I)

Summary of negative pion yield measurements. The subscript in parenthesis denotes: I = one interaction length; L = as function of target thickness; T = 0.25" target.

TABLE II: SUMMARY OF RESULTS OF PION PRODUCTION MEASUREMENT

P(P) GEV/C	P(PI) MEV/C	TARGET INCHES	0 DEGREES YIELD	0 DEGREES ERROR	0 DEGREES E/PI	10 DEGREES YIELD	10 DEGREES ERROR	10 DEGREES E/PI	20 DEGREES YIELD	20 DEGREES ERROR	20 DEGREES E/PI	30 DEGREES YIELD	30 DEGREES ERROR	30 DEGREES E/PI
6	200	,25(CU)	,009	,001	59,09	,010	,001	1,59	,008	,001	.76	.008	,001	,61
6	200	1,25(CU)	,032	,002	46,28	,036	,002	4,75	,030	,002	2.35	,031	,003	1,17
6	200	3,07(CU)	,055	,005	19,42	,058	,003	3,95	,052	,003	1,94	,048	,004	1,41
6	200	6,00(CU)	,059	,005	5,27	,076	,004	2,16	,079	,004	1,11	,089	,008	,74
6	200	12,30(CU)	,043	,003	4,53	,077	,005	2,30	,107	,005	1,50	,127	,006	1,07
17	200	,25(CU)	,024	,003	11,39	,024	,002	2,16	,021	,003	1,01	,015	,002	,58
17	200	1,25(CU)	,079	,006	25,11	,105	,006	5,43	,065	,004	3.06	,051	,004	1,61
17	200	3,07(CU)	,143	,025	41,49	,156	,009	8,80	,139	,008	3,24	,109	,012	1,79
17	200	4,30(CU)	,187	,027	31,20	,193	,011	8,48	,153	,010	3,57	,147	,015	1,57
17	200	6,00(CU)	,201	,018	18,12	,220	,020	5,05	,181	,010	2,20	,195	,017	,87
17	200	7,25(CU)	,207	,033	24,21	,248	,016	5,44	,224	,060	3,41	,206	,027	1,27
17	200	9,00(CU)	,220	,021	19,48	,253	,021	7,96	,286	,022	3,31	,346	,017	1,17
17	200	12,30(CU)	,145	,019	20,97	,265	,018	5,85	,278	,028	3,20	,343	,038	1,42
17	200	,25(W)	,019	,003	11,71	,020	,003	2,88	,018	,007	1,53	,020	,003	,59
17	200	,80(W)	,096	,009	24,53	,110	,009	5,44	,085	,011	2,27	,084	,010	,68
17	200	2,00(W)	,177	,026	13,66	,200	,014	3,26	,148	,011	1,12	,146	,020	,53
17	200	3,07(W)	,186	,020	7,05	,165	,012	2,10	,162	,012	.54	,165	,020	,28
17	200	4,00(W)	,205	,023	6,73	,256	,024	1,53	,269	,018	.33	,185	,020	,41
17	200	8,00(W)	,157	,016	4,47	,223	,021	,93	,217	,015	,35	,240	,026	,17
6	150	11,00(AL)	,030	,006	55,70	,048	,005	7,56	,049	,005	3,24	,055	,004	1,04
6	200	11,00(AL)	,065	,004	29,51	,075	,007	3,94	,057	,004	2,00	,077	,008	,61
6	250	11,00(AL)	,090	,011	23,30	,011	,001	2,02	,115	,025	,89	,137	,016	,29
6	300	11,00(AL)	,085	,017	24,69	,139	,018	1,50	,233	,015	,35	,153	,007	,22
6	350	11,00(AL)	,053	,030	31,90	,152	,016	1,16	,212	,013	.37	,143	,007	,19
6	150	6,00(CU)	,028	,005	15,96	,038	,005	6,21	,050	,005	2,23	,054	,005	1,74
6	200	6,00(CU)	,059	,005	5,27	,076	,004	2,16	,079	,004	1,11	,089	,008	,74
6	250	6,00(CU)	,104	,012	2,85	,109	,011	1,16	,126	,013	.40	,130	,009	,32
6	300	6,00(CU)	,108	,010	2,13	,140	,006	,65	,155	,009	.25	,144	,006	,24
6	350	6,00(CU)	,139	,011	1,22	,156	,008	,40	,156	,008	.27	,131	,006	,22
6	150	3,07(W)	,036	,004	3,49	,037	,003	1,94	,046	,003	,67	,042	,003	,47
6	200	3,07(W)	,062	,004	1,64	,067	,005	,66	,054	,006	.35	,058	,005	,21
6	250	3,07(W)	,088	,005	,90	,103	,006	,30	,101	,005	.16	,088	,006	,08
6	300	3,07(W)	,112	,006	,61	,106	,006	,25	,113	,006	.16	,092	,006	,11
6	350	3,07(W)	,117	,010	,49	,122	,007	,19	,111	,007	.08	,093	,006	,08
12	150	6,00(CU)	,107	,030	24,58	,089	,027	11,92	,088	,026	4.76	,111	,018	2,60
12	200	6,00(CU)	,144	,016	11,20	,158	,016	3,57	,152	,013	1,61	,157	,022	1,00
12	250	6,00(CU)	,229	,032	5,24	,247	,045	1,79	,274	,090	.64	,280	,062	,35
12	300	6,00(CU)	,263	,026	4,23	,336	,034	1,02	,465	,034	.29	,336	,021	,25
12	350	6,00(CU)	,305	,034	2,64	,293	,026	,77	,375	,028	.30	,267	,021	,18
17	150	11,00(AL)	,094	,013	61,58	,120	,012	14,50	,103	,010	4.62	,112	,010	1,57
17	200	11,00(AL)	,176	,035	29,90	,171	,021	7,77	,126	,012	3.04	,116	,017	,92
17	250	11,00(AL)	,248	,035	17,58	,279	,040	3,86	,320	,089	.97	,247	,057	,46
17	300	11,00(AL)	,337	,070	11,22	,455	,069	1,92	,611	,055	.43	,386	,036	,22
17	350	11,00(AL)	,395	,085	8,11	,492	,084	1,63	,611	,061	,34	,363	,041	,19
17	150	6,00(CU)	,146	,020	35,55	,101	,015	14,95	,118	,014	4,90	,168	,017	1,52
17	200	6,00(CU)	,201	,018	18,12	,220	,020	5,05	,181	,010	2,20	,195	,017	,87
17	250	6,00(CU)	,370	,043	8,19	,394	,053	1,80	,360	,103	.73	,306	,055	,37
17	300	6,00(CU)	,387	,062	6,14	,412	,055	1,29	,624	,143	,34	,369	,085	,28
17	350	6,00(CU)	,413	,103	4,76	,566	,049	,71	,638	,034	,25	,427	,029	,17
17	150	3,07(W)	0,000	-0,000	0,00	,165	,012	3,26	,129	,010	1,36	,133	,009	,48
17	200	3,07(W)	,186	,020	7,05	,165	,012	2,10	,162	,012	,54	,165	,020	,28
17	215	3,07(W)	,245	,029	5,94	,206	,023	1,68	,202	,015	,47	,193	,015	,20
17	250	3,07(W)	,324	,025	3,43	,323	,023	,79	,363	,062	,18	,243	,030	,13
17	300	3,07(W)	,330	,035	2,18	,423	,022	,43	,430	,035	,15	,273	,026	,10
17	350	3,07(W)	,444	,037	1,58	,435	,027	,30	,405	,026	.11	,303	,015	,06
12	200	,25(CU)	,015	,001	8,28	,020	,002	1,79	,014	,001	1,23	3,258	,293	,64
12	350	,25(CU)	,036	,005	2,73	,040	,006	,66	,027	,002	.37	,011	,002	,23

P(P) = Proton Momentum
P(PI) = Pion Momentum
Yield in pions/sr/(GeV/c)/incident proton
Error in pions/sr/(GeV/c)/incident proton
E/PI = number of electrons per pion
AL = aluminum, Cu = copper, W = tungsten

TABLE III

SOME SOURCES OF NEGATIVE PIONS

Accelerators	Maximum Protons/sec.	rads/min. in $100cm^2$ field
LAMPF	6×10^{15}	35
A.G.S.	6×10^{12}	24
Z.G.S.	1.2×10^{12}	2
Bevatron	1.4×10^{12}	1